

A Novel Current Controller Scheme for Doubly Fed Induction Generators

DOI 10.7305/automatika.2015.07.766
 UDK 621.313.333:621.316.7

Original scientific paper

This paper presents a novel current control methodology for grid connected doubly-fed induction generator (DFIG) based wind energy conversion systems. Controller is based on a proportional controller with additional first order low pass filter disturbance observer which estimates the parameter dependent nonlinear feed-forward terms. The results in simulations and experimental test bed obviously demonstrate that decoupled control of active and reactive power is achieved without the necessity of additional machine parameter.

Key words: DFIG, Disturbance observer, Wind energy

Novi regulator struje za dvostrano napajani asinkroni generator. U ovom radu prikazana je nova metoda upravljanja strujom za vjetroagregat s dvostrano napajanim asinkronim generatorom spojen na mrežu. Regulator se temelji na proporcionalnom regulatoru uz dodatak niskopropusnog filtra prvog reda za estimaciju poremećaja koji estimira parametarski ovisne nelinearne predupravljačke članove. Simulacijski i eksperimentalni rezultati pokazuju da je postignuto raspregnuto upravljanje radnom i jalovom snagom bez potrebe za dodatnim parametrima generatora.

Ključne riječi: DFIG, observer poremećaja, energija vjetra

NOMENCLATURE

i_{sa}, i_{sb}, i_{sc}	Stator a, b and c phase currents
$i_{sd}, i_{sq}, i_{rd}, i_{rq}$	Stator, rotor d and q axis currents
i_{ra}, i_{rb}, i_{rc}	Rotor a, b and c phase currents
v_{sa}, v_{sb}, v_{sc}	Stator a, b and c phase voltages
$v_{s\alpha}, v_{s\beta}, v_{r\alpha}, v_{r\beta}$	α, β axis stator, rotor voltages
v_{ra}, v_{rb}, v_{rc}	Rotor a, b and c phase voltages
$v_{sd}, v_{sq}, v_{rd}, v_{rq}$	Stator, rotor dq axis voltages
R_s, R_r	Stator, rotor resistances
P_s, Q_s	Stator active and reactive power
L_s, L_r, L_m	Stator, rotor, mutual inductances
L_{rb}	Base value of rotor inductance
ΔL_r	Disturbance of L_r
p	Number of pole pairs
ω_s, ω_r	Stator, rotor electrical speed
ω_m	Rotor mechanical speed
T_m, T_e	Mechanical and electrical torque
θ_s, θ_r	Stator, rotor electrical angle
T_s	Sample time
k_{rd}, k_{rq}	Proportional gain of controller
f_d, f_q	Disturbance terms of RSC

T_e, T_{wind}	Electrical and wind Torque
J	Inertia Constant

1 INTRODUCTION

Doubly fed induction generator (DFIG) based wind turbines are widely used in wind energy conversion systems due to their more efficient 4-quadrant active and reactive power capability and reduced converter cost compared to other variable speed wind turbine topologies, such as squirrel cage induction or synchronous generators with full scale inverters.

Conventional grid connected DFIG control strategies are usually based on stator flux [1] or voltage orientation [2] by aligning d-axis of the synchronously rotating reference frame along with the stator flux or voltage vector respectively. Control of stator power is achieved by controlling decoupled rotor currents with a classical proportional-integral (PI) current controllers. However, performance of these conventional techniques depends on accurate knowledge of machine parameters such as stator and rotor resistances and inductances which may degrade according to physical conditions. In addition to above problems, stator flux oriented methods require integral calculation and

additional band-pass filters [1] to reduce DC offsets. A comparative study between stator flux and voltage oriented methods in [3] claims that controller performances of those methods are equivalent.

DFIG based wind turbines are very sensitive to grid voltage problems due to direct connection of stator windings to the grid [4]. Robustness of the DFIG control structure against grid voltage problems and parameter variations is very crucial due to increasing power penetration from DFIG in electrical networks. Wind turbines are required to be connected to the grid with regard to low order grid voltage unbalances according to international grid and harmonic standards, such as given in [5, 6].

Direct Power Control (DPC) techniques which control machine power without the necessity of inner rotor current control loops [7, 8] are robust against parameter deviations and grid voltage disturbances. There are reputable studies which use DPC techniques [9-11] that system performance is independent on machine parameters and robust against grid voltage problems. One drawback for DPC technique is that the control structure generates variable switching frequency which complicates the power circuit design. A constant switching frequency DPC scheme is proposed in [12]. Another problem of DPC is high frequency current oscillations [13] due to high bandwidth of the controllers.

Several contributions are also encountered which use sliding mode control (SMC). Energy maximization and robustness against voltage disturbances are achieved in [14] by using second order SMC. A first order SMC is given in [15] which can operate in unbalanced and harmonically distorted grid voltages. Another second order SMC given in [4] achieves smooth connection of DFIG to the grid. Constant switching frequency second order SMC is achieved in [16]. There are also some other reputable studies which consider robustness against grid voltage problems [17] by proposing different phase-lock-loop (PLL) techniques to detect the voltage signal.

Synchronization of DFIG to the grid is another important procedure that needs to be considered. Grid and generated stator voltages must be equal in phase and amplitude before DFIG is connected to the grid. Majority of the reported schemes focus on an operation that DFIG is already connected to the grid. Synchronization procedure is deeply analyzed in [4, 18].

Grid connected DFIG control system basically consists of a back to back voltage source inverter circuit. The grid side control (GSC) circuit regulates the DC link voltage regardless of the direction of the power flow, while rotor side control (RSC) manages the stator power flow by controlling the rotor currents. Reputable studies are also encountered for GSC. Important references are summarized in [21, 22]. LCL filters design reduces the size of input inductance to reduce harmonics [23]. PLL structures which

are robust against voltage unbalances and disturbances are given in [24].

Despite the robustness of the control strategies summarized above, conventional cascaded vector controllers given in [1,2] are still popular due to simpler applicability compared to DPC and SMC methods in real systems. This study proposes a simpler novel current controller compared to previous conventional studies given in [1, 2]. Machine parameter dependent nonlinear feed-forward terms are estimated with the help of first order low pass filter disturbance observer [19]. Therefore, the necessity of accurate knowledge of the machine parameters which may deteriorate according to physical conditions is not required. Decoupled proportional current controllers are sufficient to separately control stator active and reactive power flow in RSC.

The proposed RSC scheme is implemented in a Matlab/Simulink platform and it is shown that nonlinear feed-forward terms are correctly estimated by using first order low pass filter disturbance observer. The effectiveness of the RSC controller is validated in DFIG experimental test bed by achieving decoupled control of P_s and Q_s .

The rest of the paper is organized as follows. Design of RSC current controller is explained in chapter 2. Simulation results to demonstrate the accurate estimation of disturbance terms are given in chapter 3. Experimental results for RSC controller is given in chapter 4. Finally, 5th chapter gives the conclusion and proposes the future work.

2 ROTOR SIDE CONTROL (RSC)

2.1 DFIG Dynamic Equations

DFIG dynamic equations could be written from the equivalent circuit in synchronously rotating dq frame from Fig. 2. For more detailed analysis and modeling of DFIG one can refer several numbers of sources in literature e.g. [25, 26].

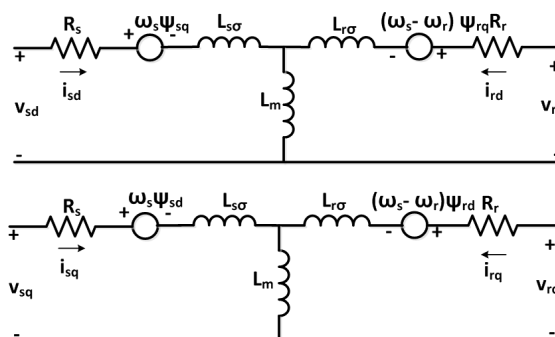


Fig. 1. DFIG Equivalent Circuit

DFIG rotor dynamics could simply be defined in the

following form:

$$L_r \frac{di_{rd}}{dt} = v_{rd} - R_r i_{rd} + \omega_r \psi_{rq} - L_m \frac{di_{sd}}{dt} \quad (1)$$

$$L_r \frac{di_{rq}}{dt} = v_{rq} - R_r i_{rq} - \omega_r \psi_{rd} - L_m \frac{di_{sq}}{dt} \quad (2)$$

Controller structure is designed in voltage oriented synchronously rotating dq frame, and the d-axis component is aligned with stator voltage vector, which mathematically means that $v_s = v_{sd}$ and $v_{sq} = 0$. All rotor variables are referred to the stator side. L_r could be divided into two values as follows;

$$L_r = L_{rb} + \Delta L_r \quad (3)$$

L_{rb} is the nominal inductance value of the rotor. ΔL_r could be treated as disturbed parameter variations due to physical effects in time and inaccuracy of its determination.

Rotor dynamic equations in (1) and (2) could be rewritten as given below. The purpose of rewriting rotor equations is to separate linear and parameter dependent nonlinear disturbance terms.

$$\frac{di_{rd}}{dt} = \frac{v_{rd}}{L_{rb}} - \underbrace{\frac{R_r}{L_{rb}} i_{rd} + \frac{\omega_r \psi_{rq}}{L_{rb}} - \frac{L_m}{L_{rb}} \frac{di_{sd}}{dt}}_{f_d^{dis}} - \frac{\Delta L_r}{L_{rb}} \frac{di_{rd}}{dt} \quad (4)$$

$$\frac{di_{rq}}{dt} = \frac{v_{rq}}{L_{rb}} - \underbrace{\frac{R_r}{L_{rb}} i_{rq} - \frac{\omega_r \psi_{rd}}{L_{rb}} - \frac{L_m}{L_{rb}} \frac{di_{sq}}{dt}}_{f_q^{dis}} - \frac{\Delta L_r}{L_{rb}} \frac{di_{rq}}{dt} \quad (5)$$

The terms, f_d^{dis} and f_q^{dis} in (4), (5) are parameter dependent nonlinear part of the DFIG rotor equations.

Stator active and reactive power equations are given as:

$$P_s = \frac{3}{2} (v_{sd} i_{sd} + v_{sq} i_{sq}) \quad (6)$$

$$Q_s = \frac{3}{2} (v_{sq} i_{sd} - v_{sd} i_{sq}) \quad (7)$$

Motion of equation can be simply defined by the following equation:

$$\frac{d\omega_m}{dt} = \frac{1}{J} (T_{wind} - T_e + b\omega_m) \quad (8)$$

2.2 Rotor Current Controller Design

If rotor currents are assumed to be measured, derivative of errors for rotor currents can be written as follows:

$$\frac{d\varepsilon_{rd}}{dt} = \frac{di_{rd}}{dt} - \frac{di_{rd}^{ref}}{dt} \quad (9)$$

$$\frac{d\varepsilon_{rq}}{dt} = \frac{di_{rq}}{dt} - \frac{di_{rq}^{ref}}{dt} \quad (10)$$

If (1) and (2) are written into (9) and (10), the following equations could be obtained:

$$\frac{d\varepsilon_{rd}}{dt} = -\frac{v_{rd}}{L_{rb}} + \underbrace{\left(\frac{di_{rd}^{ref}}{dt} + f_d^{dis} \right)}_{v_{rd}^{dis}} \quad (11)$$

$$\frac{d\varepsilon_{rq}}{dt} = -\frac{v_{rq}}{L_{rb}} + \underbrace{\left(\frac{di_{rq}^{ref}}{dt} + f_q^{dis} \right)}_{v_{rq}^{dis}} \quad (12)$$

The terms v_{rd}^{dis} and v_{rq}^{dis} are considered as parameter dependent disturbance terms which are highly nonlinear, and it is almost impossible to define the exact calculation in physical systems.

The desired closed loop dynamics can be written as follows;

$$\frac{d\varepsilon_{rd}}{dt} + k_{rd} \varepsilon_{rd} = 0 \quad (13)$$

$$\frac{d\varepsilon_{rq}}{dt} + k_{rq} \varepsilon_{rq} = 0 \quad (14)$$

The terms, k_{rd} and k_{rq} are defined as proportional gain of the rotor current controller.

If error equations in (11) and (12) are combined with desired closed loop dynamics in (13) and (14), controller voltage equations could be written as follows:

$$v_{rd} = L_{rb} (v_{rd}^{dis} + k_{rd} \varepsilon_{rd}) \quad (15)$$

$$v_{rq} = L_{rb} (v_{rq}^{dis} + k_{rq} \varepsilon_{rq}) \quad (16)$$

Nominal value of the inductance value (L_{rb}) is a constant variable, and the effect of L_{rb} could be considered as negligible in disturbance terms. Therefore, voltage equations are finalized as follows:

$$v_{rd} = v_{rd}^{dis} + L_{rb} k_{rd} \varepsilon_{rd} \quad (17)$$

$$v_{rq} = v_{rq}^{dis} + L_{rb} k_{rq} \varepsilon_{rq} \quad (18)$$

Rotor voltage references are clearly defined. Because of the constancy of L_{rb} value, controller structure is not affected from L_r variations. In addition, k_{rd} and k_{rq} values are determined by using trial and error methods in this scheme. It could be noted that the controller structure is not sensitive to any parameter accuracy.

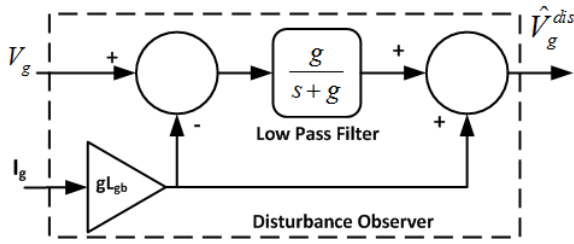


Fig. 2. Disturbance Observer Block Diagram

2.3 Design of First Order RSC Disturbance Observer

Before starting disturbance observer design concept, it is assumed that disturbance terms are bounded and can be modeled as output of known dynamical system with unknown initial conditions [19]. Besides, inputs and outputs of the system (v_{rd} , v_{rq} and i_{rd} , i_{rq}) are assumed to be measured.

Disturbance terms in (17) and (18) could be estimated by using first order low pass filter disturbance observer by rewriting rotor dynamic equations given in (1) and (2):

$$v_{rd}^{dis} = v_{rd} - L_{rb} \frac{di_{rd}}{dt} \quad (19)$$

$$v_{rq}^{dis} = v_{rq} - L_{rb} \frac{di_{rq}}{dt} \quad (20)$$

Writing (14) and (15) in s domain and implementing first order low pass filter disturbance observer concept [19]:

$$\hat{v}_{rd}^{dis} = (v_{rd} - sL_{rb}i_{rd}) \frac{g_d}{s + g_d} \quad (21)$$

$$\hat{v}_{rq}^{dis} = (v_{rq} - sL_{rb}i_{rq}) \frac{g_q}{s + g_q} \quad (22)$$

Eq. (21) and (22) could be rewritten and block diagram in Fig. 2 could be obtained as follows:

$$\hat{v}_{rd}^{dis} = \frac{g_d}{s + g_d} (v_{rd} + g_d L_{rb} i_{rd}) - g_d L_{rb} i_{rd} \quad (23)$$

$$\hat{v}_{rq}^{dis} = \frac{g_q}{s + g_q} (v_{rq} + g_q L_{rb} i_{rq}) - g_q L_{rb} i_{rq} \quad (24)$$

The terms g_d and g_q are the cut-off frequency of the low pass filter in radians. Cut-off frequency terms g_d and g_q are both selected in trial and error methods in this scheme.

The estimation error can be expressed as:

$$v_{rd}^{dis} - \hat{v}_{rd}^{dis} = \left(1 - \frac{g_d}{s + g_d}\right) v_{rd}^{dis} \quad (25)$$

$$v_{rq}^{dis} - \hat{v}_{rq}^{dis} = \left(1 - \frac{g_q}{s + g_q}\right) v_{rq}^{dis} \quad (26)$$

The estimation error converges to zero. The terms \hat{v}_{rd}^{dis} and \hat{v}_{rq}^{dis} are parameter dependent estimated disturbance

Table 1. DFIG Parameters of Simulated DFIG

	Quantity	Unit
Stator Power (P_s)	457	kW
Stator Voltage	690	V
pole number	4	-
Sync. Speed	750-78.53	rpm-rad/s
R_s	0.018	ohm
R_r	0.021	ohm
L_m	0.011	Volt
L_s	0.012	H
L_r	0.012	H
Inertia Constant	22	kgm ²

values. It is obvious from (23) and (24) that estimated disturbance terms are independent of machine parameters. As a result of the proposed controller structure explained above, Fig. 3 could be generated. Estimated disturbance terms are fed forward to the decoupled rotor current controllers. Space vector pulse with modulation (SVPWM) could be used to generate voltage references. PI controllers in the outer loops realize the desired power or speed references. Voltage angle detection is realized by conventional three-phase synchronous reference frame phase-locked loop (3 Φ -SRF-PLL), as given in [27].

3 SIMULATION RESULTS

Simulation of the proposed RSC control strategy is carried out by using MATLAB/Simulink. The purpose of simulations is to demonstrate that nonlinear feed-forward disturbance terms are accurately estimated and proposed controller structure operates at unbalanced grid voltage. Block diagram given in Fig. 3 is used by neglecting the inverter dynamics. Ideal sinusoidal voltage references are applied to the rotor and stator circuits. PI speed controller in the outer loop is used to achieve the desired speed reference. I_{rd} reference is kept zero during simulations. DFIG dynamic equations are derived from [26] with a $25\mu s$ sample time. DFIG parameter used in simulation is given in Table 1.

Stator voltage angle is calculated by using the conventional 3- Φ -PLL algorithm given in [27]. Machine parameter dependent nonlinear feed-forward terms are estimated by first order low pass filter disturbance observer. Three different scenarios are implemented in one simulation by applying speed and torque steps at different time instants as given in Table 2.

Control parameters which are optimized with trial-error methods are in Table 3. It is experienced in simulations that low cut-off frequency value delays the convergence of the estimated disturbance terms and current controllers could operate with higher proportional gains.

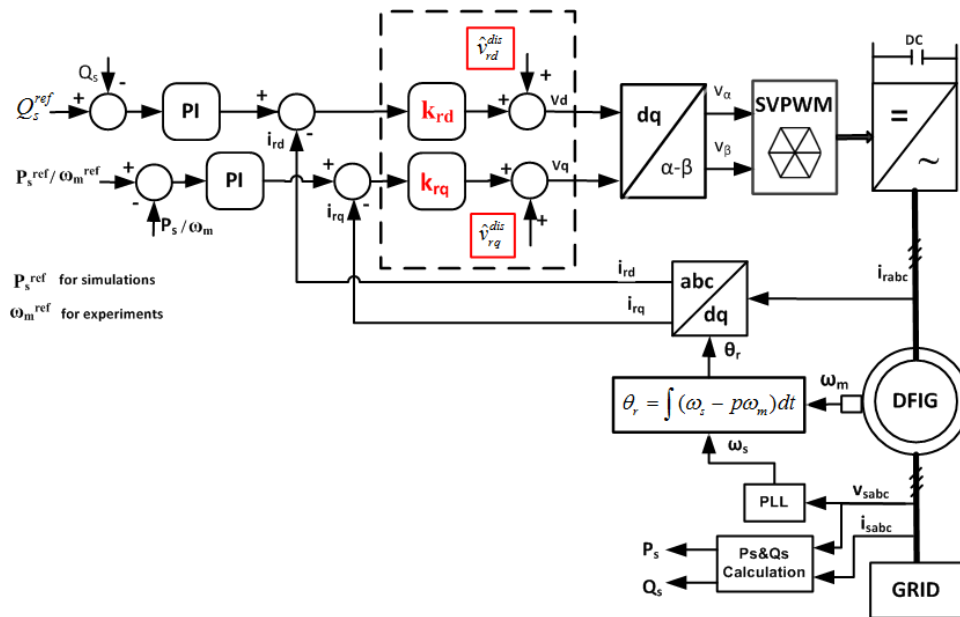


Fig. 3. Proposed RSC Scheme

Table 2. Applied Steps in Simulation

Variable	Step1	t ₁ (s)	Step2	t ₂ (s)
Speed (ω_m)	60	0-4.5	90 rad/s	4.5-20
Torque (T_e)	3000Nm	0-8	5000Nm	8-20
10% Unbalance	NO	0-14/17-20	YES	14-17
I_{rd}	0	0-20		

Table 3. Control Parameters in Simulation

Symbol	Quantity	Unit
k_{rd} and k_{rq}	5000	-
g_d and g_q	50000	radian
T_s	25	μs
Speed Controller K_p	100	-
Speed Controller K_i	250	-

Speed reference is changed from 60 to 90 rad/s (from subsynchronous to super synchronous speed) at 4.5th second. Wind torque reference is changed from 3000Nm to 5000Nm at 8th second. 10% unbalanced voltage in stator phase C is applied at 14-17th seconds.

It is expected that system must follow the speed (Fig. 4) and wind torque (Fig. 5), while accurately estimating disturbance terms. There is a huge torque and current increase at 4.5th second of simulation which is quite normal because of high torque step. Rotor d and q axis currents are shown in Fig. 6. P_s and Q_s change according to desired torque and speed references (Fig.7). The error in disturbance terms which means that difference between estimated and calculated disturbance terms are given in Fig.8-

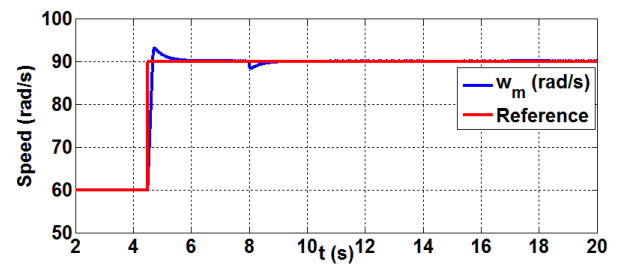


Fig. 4. Actual and reference speed

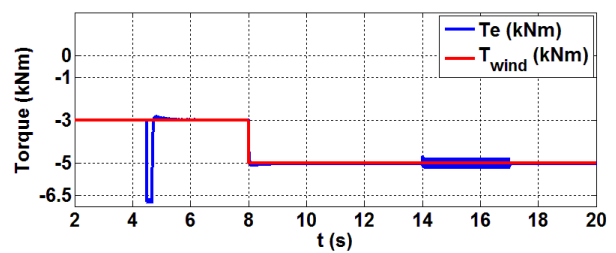


Fig. 5. Generator & Wind Torque

9. It is obvious from Fig.8-9 that estimated and calculated disturbances are equivalent. Fig. 10 demonstrates the estimated and calculated disturbance terms during 10% stator voltage unbalance in phase C for 400ms. (15-15.4 seconds).

Proposed control methodology is also compared with conventional PI current controllers as given in [2] at un-

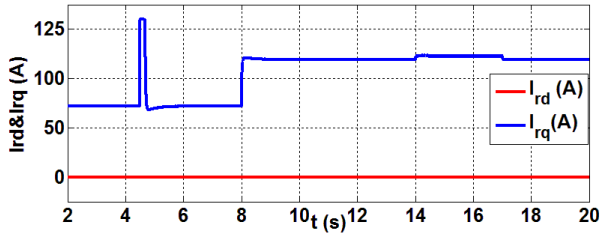


Fig. 6. Rotor currents

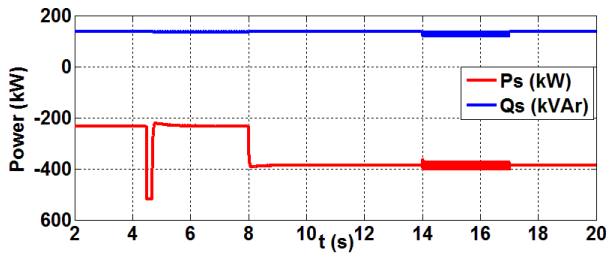


Fig. 7. P_s and Q_s variations

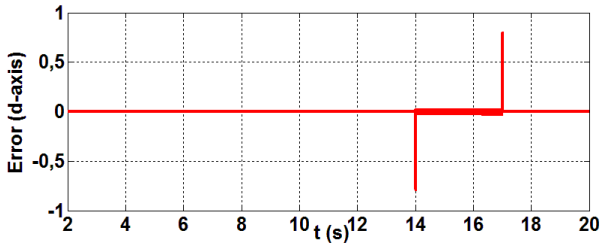


Fig. 8. Disturbance error ($\hat{v}_{rd}^{dis} - v_{rd}^{dis}$)

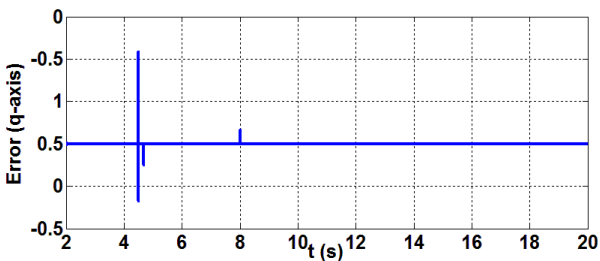


Fig. 9. Disturbance error ($\hat{v}_{rq}^{dis} - v_{rq}^{dis}$)

balanced voltage conditions. It is experienced in simulations that tuning of current PI controller gains are more complicated than the proposed method. Similar dynamic responses are achieved at certain gain values ($k_p = 0.1$ and $k_l = 12$) of PI current controllers. Control system is experienced more fragile with different controller gain values. The performance of proposed and conventional PI controller methodologies is compared at unbalanced voltage conditions. Fig.11 and 12 shows the speed responses

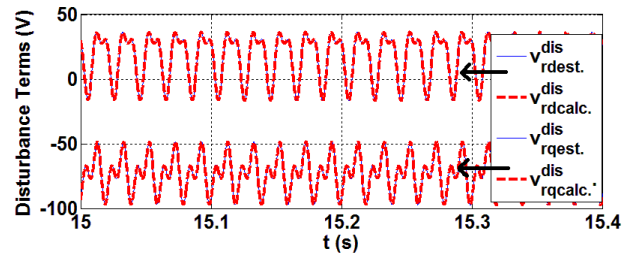


Fig. 10. \hat{v}_{rq}^{dis} & v_{rq}^{dis} terms at unbalance voltage

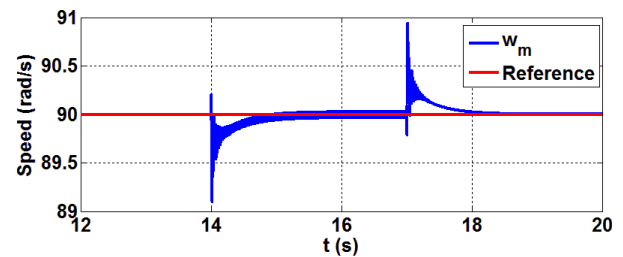


Fig. 11. Speed response of conventional method

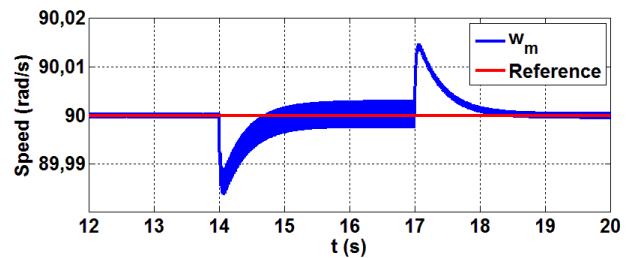


Fig. 12. Speed response of proposed method

at unbalanced voltage conditions, respectively. Fig.13 and 14 demonstrates the i_{rq} variation of conventional and proposed controller structures at unbalanced voltage conditions for 200ms. It is shown in Fig.13 that current trajectory generated by the speed controller could not be achieved in conventional method. Therefore, conventional method generates higher current oscillations. The oscillation of ω_m and i_{rq} in proposed method is reduced compared to conventional method as given in Fig.12 and 14, respectively.

4 EXPERIMENTAL RESULTS

Experimental setup in Fig. 15 is used in the experiments. A back to back inverter topology controls the rotor circuit. Squirrel cage induction machine (SCIM) is driven by a commercial inverter representing the wind. Commercial drive changes the speed of overall system. DFIG plate data is given in Table 4; gain and cut off frequency of the

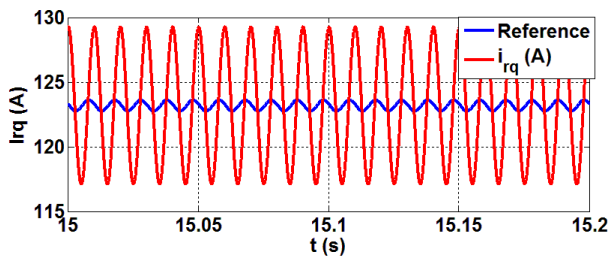


Fig. 13. I_{rq} response of conventional method

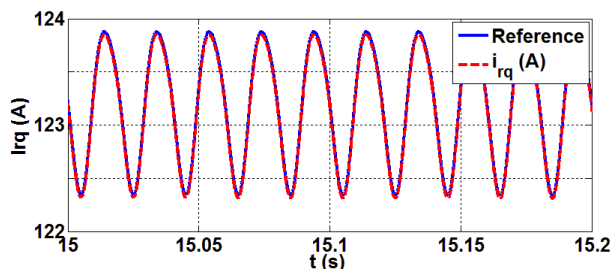


Fig. 14. I_{rq} response of proposed method

controllers are shown in Table 5. All gain and cut-off frequency values are optimized by trial and error methods. The related currents and voltages are measured and sent to the related controllers. Two separate dSPACE ds1103 controller boards are used for RSC and GSC. A classical voltage oriented vector control is used to regulate DC voltage control for GSC as given in [1]. Algorithms are generated in ControlDesk by using C programming language. Sample time of the controllers is selected as $100\mu s$. Semikron Semistack inverters are used in the experiments (21f_b6u_e1cif_b6ci_12_v12). Grid and stator voltages are separately measured for synchronization purposes. The reference of DC link voltage of GSC is kept at 120 volt in the experiments.

Table 4. DFIG Plate data in Experiments

Symbol	Quantity	Unit
Power	1.1	KW
Stator Voltage	220/380	Volt(D/Y)
Stator Current	6.4/3.7	Amper
Power Factor	0.67	-
Speed	1360	rpm
Rotor Voltage	70	Volt
Rotor Current	12	Amper

4.1 P_s and Q_s Step Response Tests

The aim of step response tests is to show that controller follows the power reference trajectory. DFIG is driven by SCIM at arbitrary speed. DC voltage reference is kept at

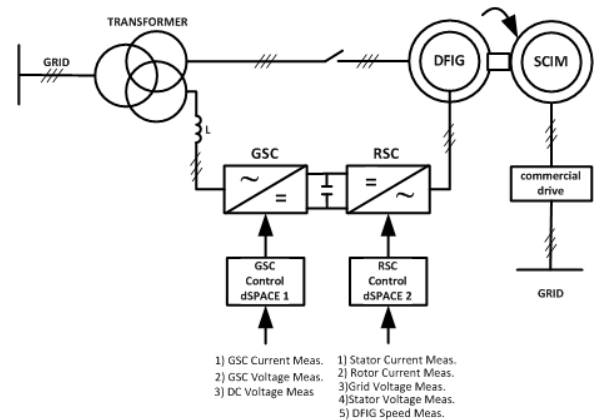


Fig. 15. Experimental Setup

Table 5. Control Parameters in Experiment

Symbol	Quantity	Unit
k_{rd} and k_{rq}	500	-
g_d and g_q	1200	radian
T_s	100	μs
f_z	10	kHz
DC Voltage	120	Volt

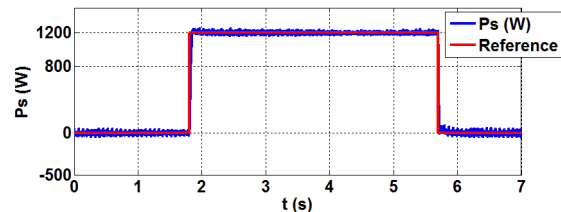


Fig. 16. P_s at P_s step response test (Exp. A)

120V by GSC. 1200 W P_s step response test is applied in Exp.A and the change of P_s and Q_s is shown in Fig. 16 and 17, respectively. Commercial drive of SCIM which represents the wind operate in open loop V/f constant control, and Fig. 18 shows that system speed decreases when this high power step response is applied. Fig. 19 shows the DC link voltage. Similarly, 160 VAr Q_s step is applied in experiment B and the change of Q_s and P_s is shown in Fig. 20 and 21, respectively.

4.2 Supersynchronous Speed Test of DFIG

The aim of supersynchronous speed test is to show that P_s and Q_s are kept stable while the speed of DFIG is changed from subsynchronous speed to supersynchronous speed. Variation of mechanical speed is shown in Fig. 22. P_s and Q_s are kept constant at 1000W and 0VAr respectively which is shown in Fig. 23 and 24, respectively. The phase change of rotor currents to supersynchronous speed

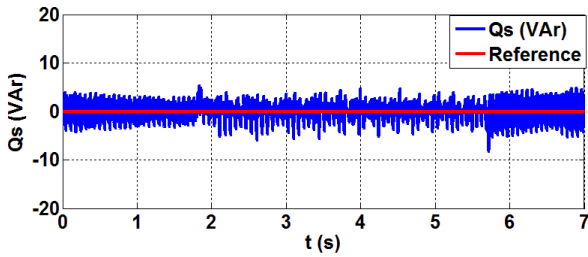


Fig. 17. Q_s at P_s step response test (Exp. A)

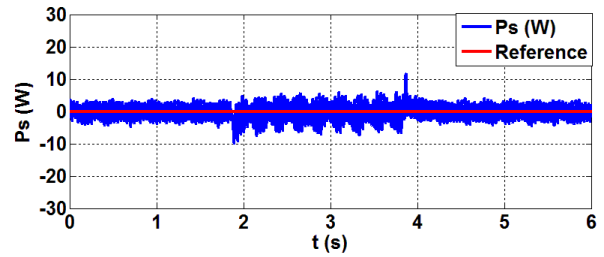


Fig. 21. P_s at Q_s step response test.

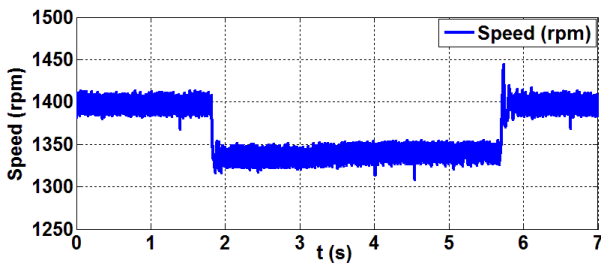


Fig. 18. ω_m at step response test (Exp.A)

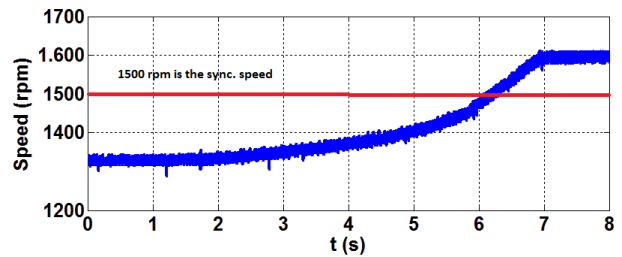


Fig. 22. Mechanical speed of DFIG

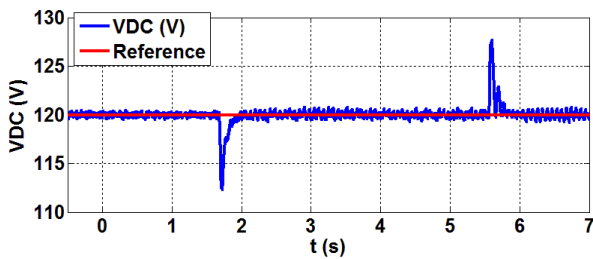


Fig. 19. DC voltage at P_s step test (Exp.A)

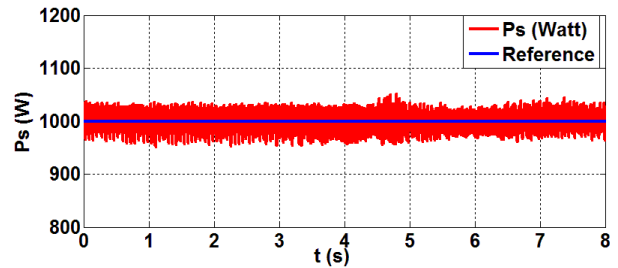


Fig. 23. P_s is kept constant at 1000W

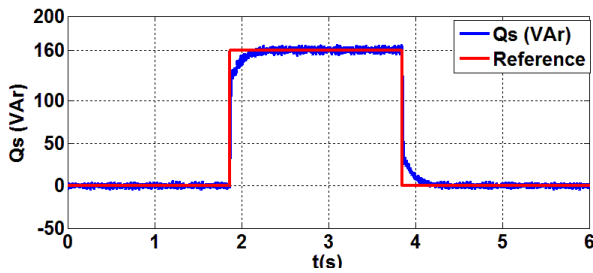


Fig. 20. Q_s at Q_s step response test (Exp. B)

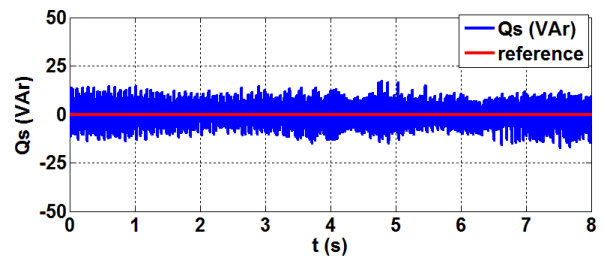


Fig. 24. Q_s is kept constant at 0VAr

is shown in Fig. 25. GSC keeps the DC link voltage constant at 120VDC which is shown in Fig.26.

5 CONCLUSION

A stator voltage oriented proportional current controllers with first order low pass filter disturbance observer has been fully demonstrated. Simulation results obviously show that proposed disturbance observer correctly

estimates the nonlinear parameter feed-forward terms and operates at unbalanced voltage conditions. The method has been validated by using experimental setup given in Fig. 15. The results in simulations demonstrate the accuracy disturbance observer in normal and unbalanced voltage conditions. The results in experiments definitely show the effectiveness of the current controllers. The proposed methodology could be applied to real DFIG based wind

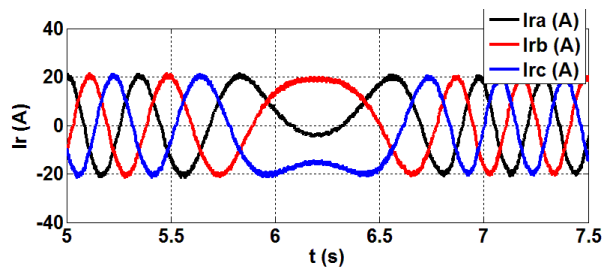


Fig. 25. Rotor Currents

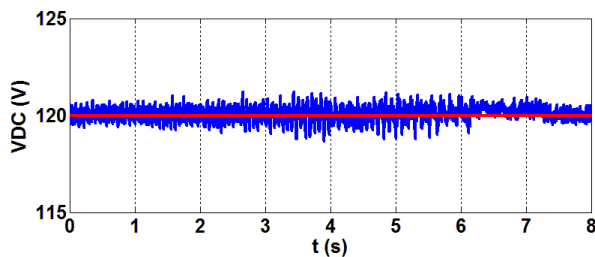


Fig. 26. DC Voltage

turbines without any complication due to its simplicity, applicability and robustness against machine parameter variations.

REFERENCES

- [1] R.Pena, J.C. Clare, and G.M. Asher, "A doubly-fed induction generator using two back-to-back PWM converters and its application to variable speed wind energy system", *Proc. Inst. Elect. Eng. B*, vol. 143, no. 3, pp. 231–241, 1996.
- [2] S. Muller, M. Deicke, and R. W. De Doncker, "Doubly fed induction generator systems for wind turbines," *IEEE Ind. Appl. Mag.*, vol. 8, no. 3, pp. 26–33, May/June 2002.
- [3] S. Li, R.Chaloo, M.J. Nemmers, "Comparative study of DFIG power control using stator-voltage and stator-flux oriented frames", *Power&Energy Society General Meeting, 2009; Canada: IEEE*, pp. 1-8..
- [4] A. Susperregui, M.I. Martinez, G.Tapia, I., Vechiu, "Second-order sliding-mode controller design and tuning for grid synchronization and power control of a wind turbine-driven doubly fed induction generator," *IET, Renewable Power Generation*, vol. 7, no. 5, pp. 540–551, Sept 2013.
- [5] IEEE 1547 *IEEE Standard for Interconnecting Distributed Resources with Electric Power Systems*, IEEE Standard 1547, 2008.
- [6] EN50160 *Voltage Characteristics in Public Distribution Systems*, European Union Standard, 2004.
- [7] L. Xu, P. Cartwright, "Direct active and reactive power control of DFIG for wind energy generation," *IEEE Trans. On Energy Conversion*, VOL. 21, No. 3, Sept. 2006.
- [8] J. Hu, H. Nian, B. Hu, Y. He and Z. Q. Zhu, "Direct Active and Reactive Power Regulation of DFIG Using Sliding-Mode Control Approach," *IEEE Trans. on Energy Conversion*, vol. 25, no. 4, Dec. 2010.
- [9] P. Zhou, J. He, and D. Sun, "Improved direct power control of a DFIG based wind turbine during network unbalance," *IEEE Trans. Power Electron.*, vol. 24, no. 11, pp. 2465–2474, Nov. 2009.
- [10] D.S. Martin, J. L.R. Amenedo, S. Arnalte, "Direct power control applied to doubly fed induction generator under unbalanced grid voltage conditions," *IEEE Transactions on Power Electronics*, Vol. 23, No. 5, pp. 2328-2336, Sep 2008.
- [11] G. Abad, M. A. Rodriguez, G. Iwanski and J. Poza "Direct power control of doubly-fed-induction-generator-based wind turbines under unbalanced grid voltage", *IEEE Trans. Power Electron.*, vol. 25, no. 2, pp.442–452 2010.
- [12] D. Zhi and L. Xu. "Direct power control of DFIG with constant switching frequency and improved transient performance". *IEEE Trans. Energy Conversion*. Vol. 22. NO. 1. Mar. 2007. pp. 110-118.
- [13] M. Mohseni, S.M. Islam, M.A.S. Masoum, "Enhanced Hysteresis-Based Current Regulators in Vector Control of DFIG Wind Turbines", *IEEE Trans. on Power Electronics*, vol. 26, no. 1, pp.223–334 Jan. 2011.
- [14] B. Beltran, M.E.H. BenBouazid, T.Ahmet-Ali, "High order sliding mode control of a DFIG based wind turbine for power maximization and grid fault tolerance," *Electric Machines and Drives Conference, 2009, IEEE International*.
- [15] I.Martinez, G. Tapia, A. Susperregui and H. Camblong, "Sliding-mode control for DFIG rotor- and grid-side converters under unbalanced and harmonically distorted grid voltage", *IEEE Trans. on Energy Convers.*, vol. 27, no. 2, pp.328–339 2012.
- [16] A. Susperregui, M.I. Martinez, I. Zubia, G. Tapia, "Design and tuning of fixed-switching-frequency second-order sliding-mode controller for doubly fed induction generator power control" *IET Electric Power Applications*, vol. 6 no. 9, pp. 696-706, 2012.
- [17] A. Luna, A. Rolan, G. Medeiros, P. Rodriguez, R. Teodorescu, "Control strategies for DFIG wind turbines under grid fault conditions," in *Proc. 35th Annual Conference of IEEE Industrial Electronics, IECON '09, 2009*.
- [18] G. Tapia, G. Santamaria, M. Telleria, A. Susperregui, "Methodology for smooth connection of doubly fed induction generators to the grid," *IEEE Trans. on Energy Conversion*, VOL. 24, No 4, Dec. 2009.
- [19] F. Blaabjerg, R. Teodorescu, M. Liserre, A.V. Timbus, "Overview of Control and Grid Synchronization for Distributed Power Generation Systems," *IEEE Transactions on Industrial Electronics*, vol.53, no.5, pp.1398-1409, Oct. 2006.
- [20] M. Carrasco, L. G. Franquelo, and J. T. Bialasiewicz, "Power Electronic Systems for the Grid Integration of Renewable Energy Sources: A Survey," *IEEE Transactions. Power Electronics*, vol. 53, No. 4, pp. 1002-1016, 2006.

- [21] M. Liserre, F. Blaabjerg, and S. Hansen, "Design and control of an LCL filter-based three-phase active rectifier," *IEEE Trans. Ind. Appl.*, vol. 41, no. 5, pp. 1281–1291, Sep./Oct. 2005.
- [22] P. Rodriguez, A. Luna, R. Teodorescu, and F. Blaabjerg, "Grid synchronization of wind turbine converters under transient grid faults using a double synchronous reference frame PLL," in *Proc. IEEE Energy 2030 Conf. (ENERGY)*, Nov. 2008, pp. 1–8.
- [23] K. Ohnishi, M. Shibata, T. Murakami, "Motion control for advanced mechatronics," *IEEE/ASME Transactions on Mechatronics*, 1(1), 56–67, March 1996.
- [24] I. Montenau, A.I. Bratcu, N.A. Cutululis, E. Ceanga, "Optimal control of wind energy systems: towards a global approach", *Advances in Industrial Control*, Springer, 2008.
- [25] W. Leonard, "Control of electric drives," 3rd Edition, Springer, Berlin, Heidelberg, New-York, 2003.
- [26] S.Chung, "A phase Tracking System for Three Phase Utility Interface Inverters", *IEEE Transactions. Power Electronics*, vol. 15, No. 3, pp. 431-438, 2000.



Eşref Emre Özsoy received the B.S. degree in electrical engineering in 2003, the M.S and Ph.D. degrees in control and automation engineering in 2008 and 2014, respectively, all from Istanbul Technical University (ITU), Istanbul, Turkey. He is currently working for an industrial company as an electrical and automation engineer. His research interests include control of electrical machines, power electronics, industrial automation and renewable energy systems.



Edin Golubovic received the B.S. degree in electrical-electronics engineering from Fatih University, Istanbul, Turkey, in 2009, and the M.S. degree and Ph.D. degree in mechatronics from Sabanci University, Istanbul, Turkey, in 2011 and 2015 respectively. Between 2009 and 2015 he has been a Teaching Assistant with the Mechatronics Program and Research Assistant with MicroMe Lab at Sabanci University, Istanbul, Turkey. His research interests include high precision motion control systems, power electronics, electrical machines control, and mechatronic systems design and integration.



Asif Sabanovic (M'92– SM'04) received the B.S. degree in electrical engineering in 1970, the M.S. and Dr.Eng. degrees in 1975 and 1979, respectively, all from the University of Sarajevo, Sarajevo, Bosnia and Herzegovina. He is a Full Professor at Sabanci University, Istanbul, Turkey. From 1970 until 1991, he was with Energoinvest Institute for Control and Computer Sciences, Sarajevo. In 1991, he was with the Department of Electrical Engineering, University of Sarajevo. During 1975–1976, he was a Visiting

Researcher with the Institute of Control Sciences, Moscow, Russia. He was a Visiting Professor with the California Institute of Technology, Pasadena, in 1984–1985, the Hitachi Chair Professor with Keio University, Yokohama, Japan, in 1991–1992, Full Professor with Yamaguchi University, Ube, Japan, in 1992–1993, Visiting Professor with the University of Maribor, Maribor, Slovenia, in 1986, 1988, and 1989, Head of Computer-Aided Design/Computer-Aided Manufacturing and Robotics Department, Tubitak—Marmara Research Centre, Istanbul, in 1993–1995, and the Head of the Engineering Department, BH Engineering and Consulting, Istanbul, in 1995–1999. His research interests include control systems, motion control systems, robotics, mechatronics, and power electronics.



Metin Gökaşan has received his BSc, M.Sc and PhD from Istanbul Technical University, Turkey in electrical and control engineering in 1980, 1982 and 1990, respectively. He is currently Professor at Electrical and Electronics Engineering Faculty and act Department Chair of at the Control Engineering in Istanbul Technical University. Between 2003 and 2006, he conducted his research at the University of Alaska Fairbanks as a visiting scholar where he worked in several

projects involving the control of HEVs and sensorless control of induction motors. His research interests are control of electrical machinery, power electronics and electrical drives, control of hybrid electric vehicles and mechatronics systems. He has authored 2 books and over 80 journal and conference publications He is a member of IEEE and Industrial Electronics Society (IES) and of the Technical Committee on Education in Engineering and Industrial Technologies in IEEE IES.



Seta Bogosyan (M'92-SM'05) has received her B.Sc., M.Sc. and Ph.D degrees in electrical and control engineering from Istanbul Technical University, Turkey in 1981, 1983, and 1991, respectively. She conducted her PhD studies at the Center for Robotics in University of California at Santa Barbara, where she worked as researcher and lecturer between 1987 and 1991. For the last decade, she has worked as associate professor at

Istanbul Technical University and is currently a faculty member at University of Alaska Fairbanks at the Department of Electrical and Computer Engineering. Her fields of interest are motion control, high efficiency control of hybrid electric vehicles, teleoperation/bilateral control systems, and applications of nonlinear control/estimation techniques to electromechanical systems in general. She has authored over a hundred journal and conference proceedings and several book chapters. She is associate editor of IEEE Transactions on Industrial Electronics (TIE), International Journal of Intelligent Automation and Soft Computing (Autosoft) and IEEE Industrial Electronics Society Magazine, (IEM). She is also a Senior Member of IEEE.

AUTHORS' ADDRESSES

Edin Golubovic, Ph.D.

Prof. Asif Sabanovic, Ph.D.

Sabanci University

Istanbul, Turkey

email: edin@sabanciuniv.edu, asif@sabanciuniv.edu

Eşref Emre Özsoy, Ph.D.

Prof. Metin Gökaşan, Ph.D.

Assoc. Prfo. Seta Bogosyan, Ph.D.

Istanbul Technical University

Istanbul, Turkey qq email: eozsoy@itu.edu.tr,

gokasan@itu.edu.tr, sbogosyan@alaska.edu

Received: 2014-02-12

Accepted: 2015-03-01